# Biomimetic motor behavior for simultaneous adaptation of force, impedance and trajectory in interaction tasks

Gowrishankar Ganesh, Alin Albu-Schäffer, Masahiko Haruno, Mitsuo Kawato and Etienne Burdet

*Abstract*— Interaction of a robot with dynamic environments would require continuous adaptation of force and impedance, which is generally not available in current robot systems. In contrast, humans learn novel task dynamics with appropriate force and impedance through the concurrent minimization of error and energy, and exhibit the ability to modify movement trajectory to comply with obstacles and minimize forces. This article develops a similar automatic motor behavior for a robot and reports experiments with a one degree-of-freedom system. In a postural control task, the robot automatically adapts torque to counter a slow disturbance and shifts to increasing its stiffness when the disturbance increases in frequency. In the presence of rigid obstacles, it refrains from increasing force excessively, and relaxes gradually to follow the obstacle, but comes back to the desired state when the obstacle is removed. A trajectory tracking task demonstrates that the robot is able to adapt to different loads during motion. On introduction of a new load, it increases its stiffness to adapt to the load quickly, and then relaxes once the adaptation is complete. Furthermore, in the presence of an obstacle, the robot adjusts its trajectory to go around it.

## I. INTRODUCTION

To interact skillfully with the environment, robots, as humans [1], [2], need to control the force and impedance at the contact points. Force provides movement and contact stability during the task while impedance helps stabilizing the system against disturbances. Most industrial manipulators use high stiffness trajectory control, as they were primarily conceived to move in the free space (e.g. to place chocolate in boxes), or were made stiff enough that the dynamic interaction can be neglected. However, modern lightweight robots will interact with fragile objects, other machines and humans [3], [4]. Such demanding and varying dynamics requires continuous adaptation of force, impedance, and, to avoid obstacles, of trajectory [5].

If a task has reproducible dynamics, suitable forces to perform it can be learned and compensated for. This is the essence of iterative and adaptive control [6], [7] which were demonstrated in implementations with various robots with nonlinear dynamics [8], [9]. However, learning forces cannot deal with unpredictable dynamics or instability. Increasing impedance is an efficient strategy to deal with incorrect forces arising from novel thus unknown dynamics, and can help perform unstable tasks, e.g. many tasks involving tool use [10]. Thus impedance control has gained popularity in recent robotics implementation, e.g. [11].

G Ganesh and E Burdet are with Imperial College of Science and Technology, UK, {gganesh; e.burdet}@imperial.ac.uk; A Albu-Schaeffer is with DLR Institute of Robotics and Mechatronics, Wessling, Germany; M Haruno is with Tamagawa University, Japan; G Ganesh and M Kawato are with ATR Computational Neuroscience Laboratories, Kyoto, Japan

While high impedance can increase stability in most movement tasks, it can lead to instability during interaction with stiff environments, expend large energy while resisting disturbances, and may cause safety issues for the robot, and objects or humans interacting with the robot [3]. In fact energy consumption is a major issue for autonomous robots, e.g. recent humanoids running on limited power from onboard batteries. Learning of the optimal forces and impedance appropriate to different tasks can help achieve them with minimum error and least energy, similar to what is seen in humans [12].

Humans have amazing ability to learn novel tasks with appropriate force and impedance, by concurrent minimization of error and energy [13], [14]. When meeting obstacles, they further modify their reference trajectory [15], thus minimizing forces. Our goal is to make robots able to perform tasks skillfully in changing dynamic interactions, by learning suitable impedance, force and trajectory.

Our recent studies [2], [12] show that human motor control fulfills about such adaptive properties. In this paper we will first formalize motor adaptation in humans as appears from our recent study [14]. We will then adapt this biomimetic controller on robots, and demonstrate it on typical robot-human interaction tasks. These include slowly changing and high frequency perturbations in postural and trajectory control tasks, as well as obstacles met during movements.

Though previous studies proposed iterative tuning of force [6], trajectory [16] and impedance [17] separately, our algorithm provides the first implementation for adapting the three simultaneously. This enables the algorithm to deal with tasks requiring adaptation of both force and impedance, and presents the unique ability to learn performing unstable tasks successfully and with minimal impedance.

## II. HUMAN MOTOR CONTROL AND LEARNING

### A. Feedforward and feedback control

To model human motor control and learning let us first analyze them from a robotics point of view. When the human hand is slightly perturbed during arm movements it tends to return to the undisturbed trajectory, as if the hand would be connected to a spring along the planned trajectory [18]. This spring-like property stems mainly from muscle elasticity and the stretch reflex, which produce a restoring force towards the undisturbed trajectory.

Further, the strength of this spring-like property, or *mechanical impedance*, increases with muscle activation [19] or with endpoint force [20], such that the damping ratio is kept constant [21]. Therefore, both stiffness and damping can
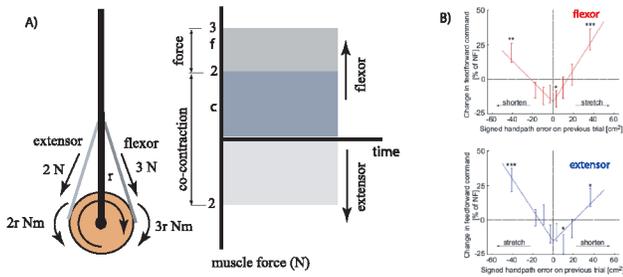
Fig. 1. **A) The cartoon of a human joint shows how the activation is achieved with multiple muscles. The difference of activation between the flexor (dark) and extensor (light grey) muscles generates the joint torque through force. Co-contraction does not contribute towards joint torque but increases impedance. B) Measured change of muscle adaptation with muscle space error [12] shows that both a positive and negative error lead to a increase of activation in both muscles. However the individual increase are different depending on the error such that the change of torque minimizes the error. Impedance (which is roughly proportional to the total muscle activation) increases irrespective of the direction of error. When the error is below a certain level impedance is decreased.**

be adapted to compensate for dynamic environments [22], though not independently.

To manipulate objects or use tools we have to interact with the environment and compensate for forces arising from it. To perform skillful control using pure feedback control with the relatively low impedance produced by musculoskeletal system, the human central nervous system (CNS) would require complex desired trajectory [20]. Further, the stabilization provided by reflexes is limited by a time delay of at least $60ms$, which means that in some cases reflexes can create instability [23]. Therefore, there must be some feedforward mechanism to plan the forces for a task in advance.

In summary, we can assume that each of the motor commands $\mathbf{w} \equiv (w_1 \cdots w_i \cdots w_N)^T$ for the $N$ muscles involved in a movement is composed of a feedforward term $\mathbf{u}$ and a feedback term $\mathbf{v}$:

$$\mathbf{w} = \mathbf{u} + \mathbf{v}. \qquad (1)$$

In contrast to most robots, humans excel in the ability to adapt rapidly to the variable dynamics of their arm as the hand interacts with the environment. Mussa-Ivaldi and his collaborators have studied this adaptation by letting subjects perform planar arm reaching movements while interacting with a velocity dependent force field [24]. They could show that the CNS adapts feedforward control during repeated trials by compensating for the environment forces, which can be modeled by nonlinear adaptive control [25], [26], [27].

However, this does not explain how humans can learn unstable tasks common in daily life, e.g. many tasks involving tool use [10]. In the last ten years, we have addressed learning of unstable tasks in humans, in a series of experimental studies, e.g. [2], [12]. We could show that humans are also able to adapt impedance independently from force by selective activation of suitable muscles groups. In summary,

humans adapt both force and impedance to perform stable and unstable tasks skillfully [28].

### B. Concurrent minimization of feedback and feedforward

Human joints are actuated by a redundant set of single directional muscle actuators, each of which can only pull, not push. The resultant activation of different muscles provides torques on the joint (Fig.1A), while muscle forces producing co-contraction are internally canceled out and do not contribute toward joint torque. However, co-activation contributes towards the joint impedance, because in each muscle impedance increases with activation [19], and impedance add in antagonist muscles, i.e. parallel actuators.

How do humans use these muscle properties to adapt to novel environments? The observations of learning patterns in [24], [2] suggest the following *principles of motor adaptation* [12]:

1) Motor commands to perform a desired action are composed of both the feedforward command, defined as the component of the motor command learned by repeating an activity, and the feedback command.
2) The feedforward command is updated from one movement to the next in muscle space as changes in the neural activation of muscles.
3) This modification of the feedforward command tends to reduce motion error experienced in the previous movement.
4) Either muscle stretch or shortening leads to augmentation of muscle activity on the following movement.
5) Muscle activation is reduced with learning.

The first principle was already formulated in (1). Motor learning consists of adapting feedforward $\mathbf{u}$ to ensure successful and optimal performance. Principles 2,3,5 mean that motor learning minimizes movement error and effort. Correspondingly we formulate motor learning as follows: the feedforward $\mathbf{u}$ depends on (positive) *activation parameters* $\mathbf{p} = (p_1, \ldots, p_N)$, which have to minimize the function:

$$V(\mathbf{p}) \equiv \frac{\alpha}{2}\mathbf{v}^T\mathbf{v} + \gamma \sum_{i=1}^{N} p_i, \quad \alpha, \gamma > 0, \qquad (2)$$

where $\mathbf{v}^T\mathbf{v}$ is a cost for movement feedback and $\sum p_i$ for the activation, i.e. for feedforward and consequently impedance. To illustrate the meaning of the activation parameter, let us now present the dynamic model structure which we will later focus on:

$$\mathbf{u}(\mathbf{p}) \equiv \mathbf{\Psi}\mathbf{p}, \qquad (3)$$

This linear function of activity parameters is a very general assumption. It includes for example the rigid body dynamics model of serial and parallel mechanisms [29], (nonlinear) adaptive control [26], neural networks and muscles synergies [30].

Corresponding to above principle 4 and experimental data (Fig.1B), for each muscle $i$, $v_i$ is an increasing function of both stretch and shortening. For simplicity we assume that this function is linearly increasing in both directions, i.e.

$$v_i = \varepsilon_{i,+} + \chi\, \varepsilon_{i,-}, \quad 0 < \chi < 1, \qquad (4)$$

where $\varepsilon_{i,+} = \max\{\varepsilon_i, 0\}$ is the positive part and $\varepsilon_{i,-} = (-\varepsilon)_{i,+}$ the negative part of the feedback error

$$\varepsilon_i = \pi(e_i + \delta\,\dot{e}_i), \quad \pi, \delta > 0, \tag{5}$$

where

$$e_i \equiv \lambda_{r,i} - \lambda_i \tag{6}$$

is the difference of muscle length $\lambda_i$ to the reference length $\lambda_{r,i}$.

We assume that learning corresponds to the gradient descent minimization of the cost function (2), i.e. activation is updated proportionally to the gradient of this function:

$$\triangle\mathbf{p}^k \equiv \mathbf{p}^{k+1} - \mathbf{p}^k \dot{=} -\frac{dV}{d\mathbf{p}}, \tag{7}$$

where $^k$ is a trial index. The gradient descent update of cost (2) is

$$\Delta\mathbf{p}^k = -\frac{dV}{d\mathbf{p}} = -\alpha\left(\frac{\partial v_i^k}{\partial p_j}\right)^T \mathbf{v}^k - \gamma\begin{bmatrix} 1 \\ \vdots \\ 1 \end{bmatrix}_N, \tag{8}$$

$w_i$ represents the environment being learned and is assumed to be independent of $p_j$, hence using $\partial w_i/\partial p_j = 0$ *for all* $(i,j)$. Equation (1) then yields:

$$\triangle\mathbf{p}^k = \alpha\left(\frac{\partial u_i}{\partial p_j}\right)^T \mathbf{v}^k - \gamma\mathbf{1}_N, \quad \alpha, \gamma > 0. \tag{9}$$

The second term, $-\gamma\mathbf{1}_N$, producing the same decrease of activation in all parameters $p_i$, is minimizing the overall activation and thus impedance in a subtle way. If activation $i$ is larger than activation $j$, then the smaller, $p_j$, is decreasing relatively faster than the larger, $p_i$. This enables learning law (9) to realize a winner-take-all scheme selecting the activation directions that were increased most from $\alpha\left(\frac{\partial u_i}{\partial p_j}\right)^T \mathbf{v}$. In the initial trials, the feedback error is large and most of the activation modification results from $\alpha\left(\frac{\partial u_i}{\partial p_j}\right)^T \mathbf{v}$. Later in the learning, optimization of impedance is performed from the term $-\gamma\mathbf{1}_N$, producing large decrease of impedance in the directions less activated, i.e. the direction of small impedance.

*C. Learning law*

We focus on the case that the motor command is linear in the activity parameters (3). With this structure the learning law (9) yields

$$\triangle\mathbf{p}^k \equiv \alpha\,\boldsymbol{\Psi}(\mathbf{s})^T \mathbf{v}^k - \gamma\,\mathbf{1}_N, \tag{10}$$

where $\mathbf{s}$ is the state. We recognize the term $\alpha\boldsymbol{\Psi}^T\mathbf{v}$ of traditional nonlinear adaptive control [7], which is now in muscle space (instead of nonredundant joint or hand space for traditional adaptive control).

In contrast to traditional adaptive control of force, the feedforward will continue to be adapted even when the error is 0, as energy is now minimized concurrently to error. However, muscles can only pull and not push, and they are naturally bounded by a minimum positive pull value.

Note that the update of each activation depends only on the error and is independent on the other activations, i.e. no explicit dependence between the activations is needed to regulate endpoint force and impedance with the coupled and highly nonlinear dynamics of a redundant multi-neuron, multi-muscle, multi-joint system.

How do the force and impedance vary with this scheme? The adaptation law (10), with the asymmetric V-shaped feedback error (4), can be decomposed into an antisymmetric proportional function of the feedback error, a symmetric function and a negative bias:

$$\begin{aligned} \triangle\mathbf{p}^k &= \alpha\boldsymbol{\Psi}^T\varepsilon_+^k + \alpha\chi\boldsymbol{\Psi}^T\varepsilon_-^k - \gamma\mathbf{1}_N \tag{11} \\ &= \frac{\alpha}{2}(1-\chi)\boldsymbol{\Psi}^T\varepsilon^k + \frac{\alpha}{2}(1+\chi)\boldsymbol{\Psi}^T|\varepsilon^k| - \gamma\mathbf{1}_N, \end{aligned}$$

where

$$|\boldsymbol{\varepsilon}| \equiv (|\varepsilon_1|, \ldots, |\varepsilon_i|, \ldots, |\varepsilon_N|) \tag{12}$$

is defined componentwise. As it was shown in [12] that a deviation to one direction is compensated for by a force in the opposite direction in the next trial (principle 3), hence $\chi < 1$. In this representation, the first term in $\varepsilon$ produces a force opposed to the error, i.e. compensates for systematic error, the second term in $|\varepsilon|$ increases co-activation in response to deviation, i.e. increases stability, and the third term $-\gamma\mathbf{1}_N$ removes superfluous (co-)activation. Therefore, *the adaptation of (10) concurrently increases stability, decreases movement error and decreases effort*.

The first term produces a modification of reciprocal activation, and corresponds to the force regulation algorithms of nonlinear adaptive control [7], iterative control [6], and previous models of motor learning [25], [26], [27]. The other terms tune the co-activation in all antagonist muscles groups, i.e. our scheme is extending these algorithms to simultaneous regulation of force and impedance.

## III. AUTOMATIC MOTOR BEHAVIOR FOR ROBOTS

In adaptive control [8], [9] index $^k$ corresponds to time, i.e. the dynamic model $\boldsymbol{\Psi}\mathbf{p}$ is modified during motion. Here we will illustrate the possibility of this human motor control model when movements are repeated trial after trial, i.e. for iterative control [6], [9]. In this case $^k$ corresponds to the trial number and (3) reduces to $\mathbf{u} \equiv \mathbf{p}$, thus $\boldsymbol{\Psi} \equiv \mathbf{1}$.

Similar to the human controller (1), the robot controller involves feedforward and feedback, where now $\mathbf{w}$ stands for the overall control torque, $\mathbf{u}$ is feedforward torque, and feedback error is

$$\mathbf{v}^k \equiv \mathbf{K}^k\mathbf{e}^k + \mathbf{D}^k\dot{\mathbf{e}}^k, \quad \mathbf{e}^k \equiv \mathbf{q}_r^k - \mathbf{q}^k, \tag{13}$$

where $\mathbf{q}$ represents the robot angles vector and the error signal $\mathbf{e}$ is calculated with respect to the reference $\mathbf{q}_r$.

Feedforward and mechanical impedance are adapted as in the human controller (11):

$$\triangle\mathbf{u}^k \equiv \mathbf{u}^{k+1} - \mathbf{u}^k \equiv \alpha\,\varepsilon^k, \quad \alpha > 0, \tag{14}$$

$$\triangle\mathbf{K}^k \equiv \mathbf{K}^{k+1} - \mathbf{K}^k \equiv \beta\,|\varepsilon^k| - \gamma\mathbf{1}, \quad \beta, \gamma > 0 \tag{15}$$
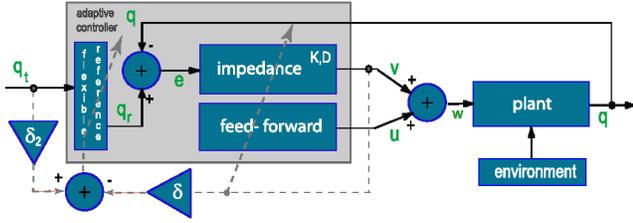
Fig. 2. **The block diagram of the adaptation algorithm elucidates the online (black lines) and learning (dashed grey lines) signals driving the adaptive feedforward, impedance and trajectory controller.**



Fig. 3. **The DLR light-weight robot (LWR) link and the coordinate system.**

Equation (14) corresponds to the first, and Equation (15) corresponds to the last two terms of Equation (11). The damping term $\mathbf{D}$ is changed as a constant relation of stiffness such that:

$$D_{ij}^k \equiv 2\sqrt{K_{ij}^k}. \tag{16}$$

However, as the robot lacks the fatigue properties of human muscles, which lead to an automatic relaxation of forces, we introduce this in (14) as:

$$\triangle \mathbf{u}^k \equiv \mathbf{u}^{k+1} - \mathbf{u}^k \equiv \alpha\,\varepsilon^k - (1-\mu)\,\mathbf{u}^k \tag{17}$$

where $\mu$ is the relaxation factor, with $\mu < 1$.

Finally, we extend the human algorithm to include trajectory adaptation. The principle behind this adaptation is the concurrent minimization of feedback and task error, giving rise to the gradient descent

$$\triangle \mathbf{q}_r^k \equiv \mathbf{q}_r^{k+1} - \mathbf{q}_r^k \equiv -\delta\,\varepsilon^k + \delta_2\,(\mathbf{q}_t^k - \mathbf{q}_r^k), \tag{18}$$

where $\delta$ and $\delta_2$ represent the positive weights of the two attractor trajectories and $\delta >> \delta_2$. The task is specified by a task trajectory $\mathbf{q}_t$, which the reference trajectory is initially equal to.

Equation (1) together with (13,15 -18) yield the control and adaptation for simultaneous control and adaptation of force, impedance and trajectory of the robot, as depicted in Fig. 2.

If we consider the adaptation of activation determining whole movements, the motor command, activation and state vector are all functions of the time: $\mathbf{u} \equiv \mathbf{u}(t)$, $\mathbf{K} \equiv \mathbf{K}(t)$, $\mathbf{q} \equiv \mathbf{q}(t)$, $\varepsilon \equiv \varepsilon(t)$, $t \in [0, T]$. In the postural case the time $t$ is reduced to an instant with $^k$ becoming the time parameter along which the evolution of all variables is performed.

We first elucidate the adaptive control in a posture control task (Section V-A) and show that it induces human-like behavior in the robot (Figs. 4, 5). This is followed by a learning experiment to show the adaptation performed by the robot to different loads during movement (Section V-B) and the trajectory adaptation observed in the presence of an obstacle (Section V-C).

## IV. ROBOTIC IMPLEMENTATION

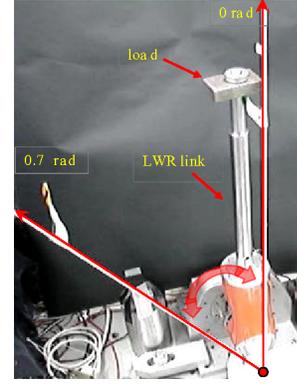The experiments were performed on a 1 DOF test-setup (Fig. 3) of the DLR light-weight robot [31]. The controllers

were implemented on a dSpace controller board with a sampling rate of 2kHz. The interface used torque feedback to compensate for joint friction and gravity, such that the joint could be regarded as a high performance torque source [11].

The parameters used for the posture control experiment were: $\alpha = 9.0$, $\beta = 0.2$, $\gamma = 0.0327$, $\delta = 6.2e^{-5}$, $\delta_2 = 2.48e^{-5}$ $\mu = 0.8$. These were chosen by trial and error so that the behavior is quantitatively similar to humans [32], but may be tuned as per requirements. The relative values of $\alpha$, $\beta$ and $\gamma$ determined the disturbance acceleration threshold at which the impedance change dominates force change and was chosen as $2rad/s^2$ (0.1 rad, 3 Hz) for this experiment. $\gamma$ also determined the rate of relaxation in the absence of perturbations and was tuned so as to make the robot relax completely in about 3 seconds. The values of $\delta$ and $\delta_2$ required to be small compared to $\alpha$ to ensure stability, while being large enough to enable a notable change in the reference trajectory in the limited experiment time. The parameter $\mu$ determines the rate of decrease of force. It is more important in the late stage of learning and can be adjusted to determine the steady state contact force.

The parameters for trajectory control experiment: $\alpha = 1.0$, $\beta = 0.95$, $\gamma = 1.5$, $\delta = 0.03$, $\delta_2 = 0.006$ and $\mu = 0.8$, were chosen in a similar manner. The chosen value of $\alpha$ ensured that the robot learns a perturbation only if it repeats for three or more trials and hence helped in rejecting noise (due to random disturbances). A relatively higher $\beta$ and $\gamma$ values were chosen in the trajectory experiment to get a fast increase in impedance in case of task errors and a fast decrease once the error in learnt.

In both implementations the stiffness $\mathbf{K}$ was bounded between $5Nm/rad$ and $100Nm/rad$.

## V. EXPERIMENTS AND RESULTS

### A. Postural control

In this experiment the robot attends to maintain its initial position at $0.05rad$ (Fig.4A) while perturbations of low (light grey in Fig.4A) or high (dark grey in Fig.4A) frequency are applied on the robot. The robot adapts to the vibration by
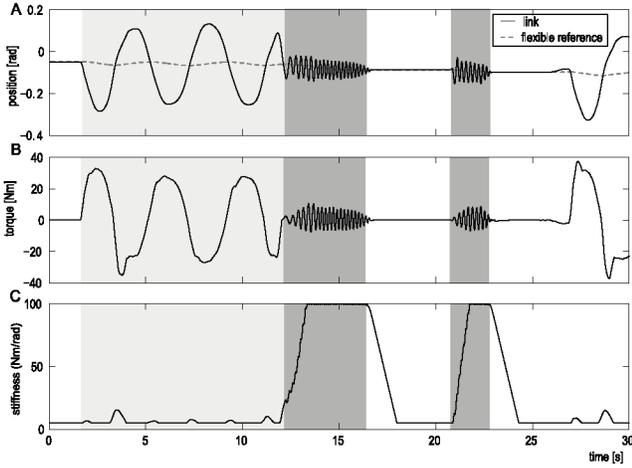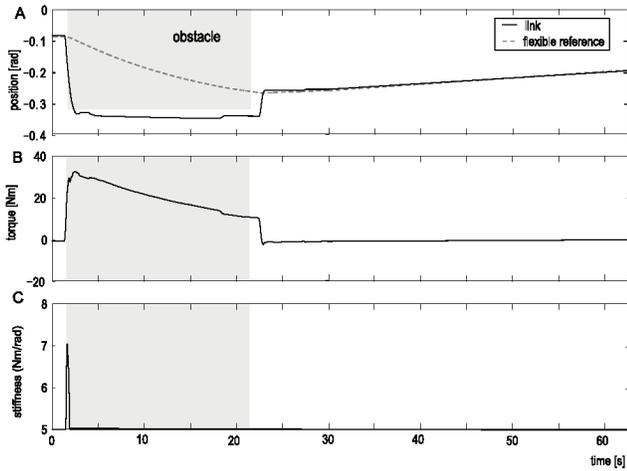
Fig. 4.   **Posture control experiment**



Fig. 6.   **Trajectory adaptation experiment.**



Fig. 5.   **Obstacle avoidance during posture control**

changing the applied torque (Fig.4B) or impedance (Fig.4C) to minimize the deviation. When the force perturbation changes slowly, the robot applies a counter torque to reduce the deviation, with little change of impedance. However, when the perturbation frequency is higher, the robot no longer counters with torque but automatically increases its stiffness to reduce the deviation. This behavior is similar to that observed in humans doing a similar task [32].

When there is a position perturbation due to an obstacle (grey section of Fig.5A), the controller immediately increases stiffness and then torque, trying to bring the robot end effector back, but after a particular level the torque is no longer increased. Instead the controller adapts the reference trajectory while reducing the torque (Fig.5B). When the obstacle is removed, the end-effector slowly moves back to the original position.

### B. Trajectory control

The second experiment tests the adaptation to loads by the robot while it aims to move repetitively between 0 radians
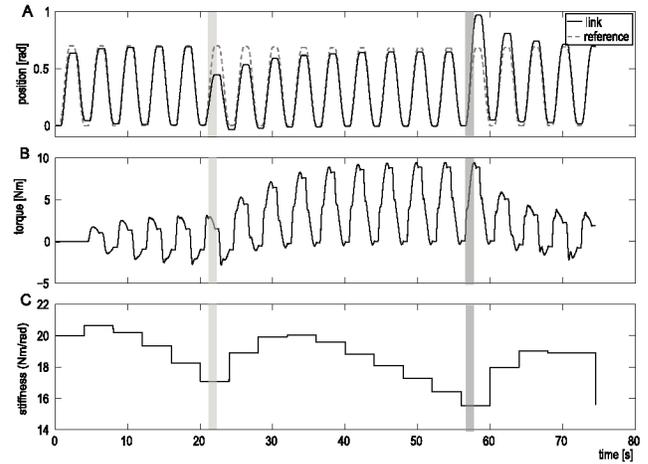
and 0.7 radians (grey dashed trace of Fig.6). The experiment starts with the robot at 0 degrees and with an unknown load fixed to the link, which causes a deviation from the reference trajectory which is reduced in 5 trials, by adaptation. In the 6th trial an extension spring is attached to the link and reduces the movement amplitude (light grey region in Fig.6A). However the robot again learns the required torque (Fig.6B) to achieve the movement task in about 9 movements. The spring is then removed in the 15th trial (dark grey region in Fig.6A), causing an overshoot, after which the robot readapts to have the torque levels similar to that before the spring addition.

Fig.6B shows the underlying torque adaptation and Fig.6C the adaptation of the stiffness of the robot during the experiment. The stiffness is initially high but the end-effector becomes more compliant as the robot adapts to the unknown load. When the spring is added, the robot increases its stiffness to adapt quickly to the error induced. However, as the robot adapts, the stiffness is reduced again. When the spring is suddenly removed, leading to an error in the task, stiffness again increases and then reduces as it is readapted.

The video file showing posture control and trajectory adaptation may be viewed at *http://www.cns.atr.jp/~gganesh/robot_learning.rar.*
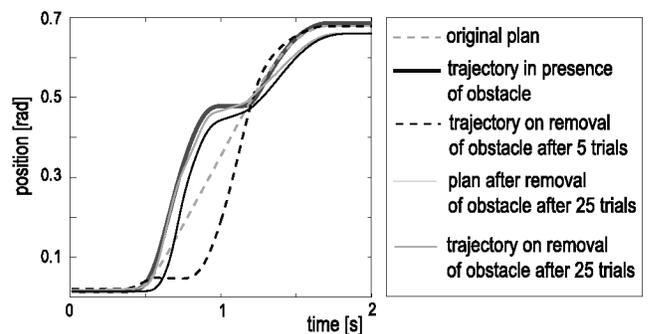


Fig. 7.   **obstacle avoidance during trajectory control.**

## C. Obstacle avoidance

In order to test the trajectory adaptation by the algorithm in the presence of an obstacle, we use a ramp up and down as obstacle (thick black trace in Fig.7) added to the original plan (dashed grey trace) of the robot movement. When the obstacle is suddenly removed in the 5th adaptation trial, the movement is reduced by as much as it was increased due to adaptation, mirroring the obstacle (dashed black trace). This behavior shows that the robot initially tries to increase the torque to counter the obstacle.

The obstacle is then re-introduced from the 6th trial on. When the obstacle is removed in the 25th trial the robot movement (black trace) and plan (grey trace) can be clearly seen to have adapted to the shape of the obstacle. The robot movement (black trace) lies to the right of the plan (grey trace), indicating that the robot still applies some contact force onto the obstacle after 25 trials. This behavior is similar to the adaptation observed in humans [15].

## VI. DISCUSSION

Robots interacting with dynamic environments require to continuously adapt their position, force and impedance depending on the requirements of the task. Traditionally this was solved using nonlinear model based control and design approaches [33], [34], [11], but due to parametric uncertainties it is difficult to get an accurate model of robot dynamics. Thus robot performance was shown to be better when the robot model is learnt during motion [9] than computed from design and material information [35]. Further, it is hard to model the interaction with an unknown environment. Unlike robot dynamics, environment dynamics may be time variant and thus require continuous model adaptation.

Robot manipulation is usually employed to perform repetitive tasks. Even if a robot, naive to its dynamics and that of its environment, is initially unsuccessful in a task, it can use the knowledge gained in previous trials to gradually improve the next one through learning of a feedforward, which corresponds to a model of the robot dynamics and its environment. This is the basic observation of motor learning in animals, including humans [24], [2], [12] and is similar to the concept of iterative learning proposed in robotics [6], [36], [9].

Forces/torques help generate robot motions while impedance is important to maintaining stability against disturbances. Adapting force and impedance as per the requirement of an environment helps maximizing interaction safety and minimizing energy consumption. Trajectory adaptation, on the other hand, helps robots to change motion depending on the changes in the environment such as the introduction of an obstacle. Though theoretically force and trajectory adaptations do not need to be considered independently, because the impedance acts about the trajectory as reference, it is practical to separate them in order to distinguish movement related forces from interaction forces.

While iterative tuning of force [6], trajectory [16] and impedance [17] were proposed separately in previous studies,

our algorithm combines iterative feed-forward learning and adaptive impedance control, to give the first implementation for adapting the three functions simultaneously. This generalizes the applications field of robots to tasks requiring simultaneous adaptation of force and impedance, e.g. most tasks performed in interaction with the environment.

Previous iterative algorithms try to converge the robot states to a predefined desired force [37], position [38], [39] or impedance [17]. In contrast, our algorithm proposes a flexible-supervised approach where the reference trajectory is not rigid and slowly changes with time so as to minimize the task error, forces and energy. Simultaneously the error with respect to the flexible reference is used to tune the force and impedance values. However our algorithm does require an initial reference trajectory at each joint. As this trajectory is kinematic, it may be ideally achieved by higher level processes like imitation learning, similar to what has been observed in humans [40].

During interaction with objects and humans, a compliant robot can provide a safe interaction for the robot and the obstacles [41], or a stable contact can be provided by control of contact forces. Task space force control [42] and impedance control [33], [11] are popular control structures proposed for such tasks. Our algorithm does not perform force control directly, but it learns to follow obstacles in a manner similar to force control, while retaining the disturbance robustness properties of impedance control. This behavior can be observed in Fig. 7 where the incomplete convergence of the reference (solid grey trace), due to the presence of two attractors (18), leads to maintenance of a contact force between the obstacle and robot. Due to the presence of this contact force, on obstacle removal, the robot movement (solid black trace) lies inside the obstacle.

The contact force on the surface in the 1 DOF case may be obtained by setting (17) and (18) to zero and is given by

$$F_c = \frac{\alpha \, K_{min} \, \delta_2}{\mu \, \delta} \, (q_t - q_r) \, L \,, \qquad (19)$$

where $K_{min}$ represents the minimum stiffness allowed for the joint and $L$ is the link length. In the case of a multi-joint system while a contact force will still be kept, its magnitude will also dependent on the robot kinematics. If required, the magnitude of the contact force can be controlled by the relative strength of the attractor trajectories of (18).

A significant advantage of our algorithm over existing impedance adaptation algorithms [17], [43] is in its ability to deal with unstable environments [28] where task error fluctuates randomly. In traditional iterative or adaptive control, as the learning is related to feedback, random trial errors in different directions can lead to the cancelation of model from the previous trials [14]. In the proposed algorithm, any error, irrespective of its direction, leads to an initial increase in impedance which helps reduce the error and promotes the iterative learning of force. Once the appropriate forces are learnt, the task error is reduced, which in turn leads to a decrease in impedance to levels which still keep the system stable. Implementation of the algorithm in a multi-

joint system has now been realized (and will be reported elsewhere) giving automatic spatial tuning of task impedance as seen in humans [2], [44], where impedance is adapted to be large only in specific directions or joints as required by the task.

## VII. Acknowledgments

## References

[1] N. Hogan, "Adaptive control of mechanical impedance by coactivation of antagonist muscles." *Automatic Control, IEEE Transactions on*, vol. 29, no. 8, pp. 681–690, 1984.

[2] E. Burdet, R. Osu, D. Franklin, T. Milner, and M. Kawato, "The central nervous system stabilizes unstable dynamics by learning optimal impedance." *Nature*, vol. 414, no. 6862, pp. 446–449, 2001.

[3] M. Peshkin and J. E. Colgate, "Cobots." *Industrial Robot*, vol. 26, no. 5, pp. 335–341, 1999.

[4] O. Lambercy, L. Dovat, R. Gassert, C. Teo, T. Milner, and E. Burdet, "A Haptic Knob for Rehabilitation of Hand Function." *IEEE Transactions on Neural Systems and Rehabilitation Engineering*, vol. 15, no. 3, pp. 256–266, 2007.

[5] E. Boy, E. Burdet, C. Teo, and J. Colgate, "Experimental Evaluation of Motion Guidance with a Cobot." *IEEE Trans Robotics*, vol. 23, no. 3, pp. 245–255, 2007.

[6] Z. Bien and J. Xu, *Iterative learning control: analysis, design, integration and applications.* Kluwer Academic Publishers, Norwell, MA, 1998.

[7] J. Slotine and W. Li, *Applied nonlinear control.* Prentice Hall Englewood Cliffs, NJ, 1991.

[8] G. Niemeyer and J. Slotine, "Performance in Adaptive Manipulator Control." *Int J Robo Res.*, vol. 10, no. 2, pp. 149–161, 1991.

[9] E. Burdet, A. Codourey, and L. Rey, "Experimental evaluation of nonlinear adaptive controllers." *IEEE Control System Magazine*, vol. 18, pp. 39–47, 1998.

[10] D. Rancourt and N. Hogan, "Stability in force-production tasks." *J Motor Behav.*, vol. 33, no. 2, pp. 193–204, 2001.

[11] A. Albu-Schäffer, C. Ott, and G. Hirzinger, "A unified passivity based control framework for position, torque and impedance control of flexible joint robots." *J Robot Res.*, vol. 26, no. 1, pp. 23–39, 2007.

[12] D. Franklin, E. Burdet, R. Osu, K. Tee, C. Chew, T. Milner, and M. Kawato, "CNS learns stable, accurate, and efficient movements using a simple algorithm." *J Neurosci.*, vol. 28, no. 44, pp. 11 165–11 173, 2008.

[13] I. 'O' Sullivan, E. Burdet, and J. Diedrichsen, "Dissociating variability and effort as determinants of coordination." *PLoS Comput Biol.*, vol. 5, no. 4, p. e1000345, 2009.

[14] K. Tee, D. Franklin, T. Milner, M. Kawato, and E. Burdet, "Concurrent adaptation of force and impedance in the redundant muscle system." *Biol Cybern.*, vol. submitted, 2009.

[15] J. L. Chib, V.S. amd Patton, K. Lynch, and F. Mussa-Ivaldi, "Haptic Identification of Surfaces as Fields of Force." *J Neurophysiol.*, vol. 95, pp. 1068–1077, 2006.

[16] P. Jiang, P. Woo, and R. Umbehauen, "Iterative learning control for manipulator trajectory tracking without any control singularity." *Robotica*, vol. 20, pp. 149–158, 2002.

[17] C. Cheah and D. Wang, "Learning Impedance Control for Robotic Manipulators." *Proc IEEE International Conference on Robotics and Automation (ICRA)*, vol. 14, no. 3, 1998.

[18] J. Won and N. Hogan, "Stability properties of human reaching movements." *Exp Brain Res.*, vol. 107, pp. 125–136, 1995.

[19] R. Kirsch, D. Boskov, and W. Rymer, "Muscle Stiffness During Transient and Continuous Movements of Cat Muscle: Perturbation Characteristics and Physiological Relevance." *IEEE Transactions on Biomedical Engineering*, vol. 41, no. 8, pp. 758–770, 1994.

[20] H. Gomi and R. Osu, "Task-Dependent Viscoelasticity of Human Multijoint Arm and Its Spatial Characteristics for Interaction with Environments." *J Neurosci.*, vol. 18, no. 21, pp. 8965–8978, 1998.

[21] E. Perreault, R. Kirsch, and P. Crago, " Multijoint dynamics and postural stability of the human arm." *Exp Brain Res.*, vol. 157, pp. 507–517, 2004.

[22] T. Milner and C. Cloutier, "Compensation for mechanically unstable loading in voluntary wrist movement." *Exp Brain Res.*, vol. 94, no. 3, pp. 522–532, 1993.

[23] A. Jacks, A. Prochazka, and P. Trend, "Instability in human forearm movements studied with feed-back-controlled electrical stimulation of muscles." *J Physiol.*, vol. 402, pp. 443–461, 1988.

[24] R. Shadmehr and F. Mussa-Ivaldi, "Adaptive representation of dynamics during learning of a motor task." *J Neurosci.*, vol. 14, no. 5, pp. 3208–3224, 1994.

[25] M. Kawato, K. Furukawa, and R. Suzuki, "A hierarchical neural-network model for control and learning of voluntary movement." *Biol Cybern.*, vol. 5, pp. 169–185, 1987.

[26] E. Burdet, "Algorithms of human motor control and their implementation in robotics." *PhD thesis, ETH-Zurich, Switzerland*, 1996.

[27] R. Sanner and M. Kosh, "A mathematical model of the adaptive control of human arm movements." *Biol Cybern.*, vol. 80, no. 5, pp. 369–382, 1999.

[28] E. Burdet, K. Tee, I. Mareels, T. Milner, C. Chew, D. Franklin, R. Osu, and M. Kawato, "Stability and motor adaptation in human arm movements." *Biol Cybern.*, vol. 94, pp. 20–32, 2006.

[29] A. Codourey and E. Burdet, "A Body-oriented Method for Finding a Linear Form of the Dynamic Equation of Fully Parallel Robots." *Proc IEEE International Conference on Robotics and Automation (ICRA)*, vol. 2, 1997.

[30] A. d'Avella, A. Portone, L. Fernandez, and F. Lacquaniti, "Control of Fast-Reaching Movements by Muscle Synergy Combinations." *J Neurosci.*, vol. 26, no. 30, p. 7791, 2006.

[31] A. Albu-Schäffer, S. Haddadin, m. Ott, A. Stemmer, T. Wimböck, and G. Hirzinger, "The DLR Lightweight Robot - Design and Control Concepts for Robots in Human Environments." *Industrial Robot*, vol. 134, no. 5, pp. 376–348, 2007.

[32] G. Ganesh, M. Haruno, and E. Burdet, "Transitions between reciprical activation and co-contraction during posture control." *Poster at Neural Control of Movement*, vol. NCM'08, 2008.

[33] N. Hogan, "Impedance control: An approach to manipulation: Part I, part II, part III." *ASME J. Dynam Syst., Meas., Contr.*, vol. 107, pp. 1–24, 1985.

[34] T. Yoshikawa, T. Sugie, and M. Tanaka, "Dynamic hybrid position/force control of robot manipulators: Controller design and experiment." *J Robot Automat.*, vol. 4, pp. 699–705, 1988.

[35] E. Burdet and A. Codourey, "Evaluation of parametric and non-parametric nonlinear adaptive controllers." *Robotica*, vol. 16, pp. 59–73, 1998.

[36] S. Arimoto, S. Kawamura, and F. Miyazaki, "Better operation of robots by learning." *J Robot Sys.*, vol. 1, no. 2, pp. 123–140, 1984.

[37] B. Qiaoa, J. Y. Zhua, and Z. X. Weia, "Learning Force Control for Position Controlled Robotic Manipulator." *CIRP Annals - Manuf Technol.*, vol. 48, no. 1, pp. 1–4, 1999.

[38] K. L. Moore, M. Dahleh, and S. P. Bhattacharyya, "Iterative learning for trajectory control." *Decision and Control, Proceedings of the 28th IEEE Conference on*, vol. 1, pp. 860–865, 1989.

[39] D. Wang and N. H. McClamroch, "Position/force control design for constrained mechanical systems: Lyapunovs direct method." *IEEE Trans. Robot. Automat.*, vol. 9, pp. 308–313, 1997.

[40] N. Shea, "Imitation as an inheritance system." *Philos Trans R Soc Lond B Biol Sci.*, vol. 368, no. 1528, pp. 2429–2443, 2009.

[41] A. Albu-Schäffer, O. Eiberger, M. Grebenstein, S. Haddadin, m. Ott, T. Wimbock, S. Wolf, and G. Hirzinger, "Soft robotics: From Torque Feedback Controlled Lightweight Robots to Intrinsically Compliant Systems." *IEEE Robotics & Automation Magazine*, pp. 20–30, 2008.

[42] O. Khatib, "A unified approach for motion and force control of robot manipulators: the operational space formulation." *IEEE J robot Autom.*, vol. 3, pp. 43–53, 1987.

[43] L. Huang, S. S. Ge, and T. H. Lee, "An adaptive impedance control scheme for constrained robots." *J Robot Automat.*, vol. 4, pp. 699–705, 1988.

[44] D. Franklin, E. Burdet, R. Osu, M. Kawato, and T. Milner, "Functional significance of stiffness in adaptation of multijoint arm movements to stable and unstable dynamics." *Exp Brain Res.*, vol. 151, pp. 145–157, 2003.